Supplemental Information

Supplemental Data:

Supplemental Figures

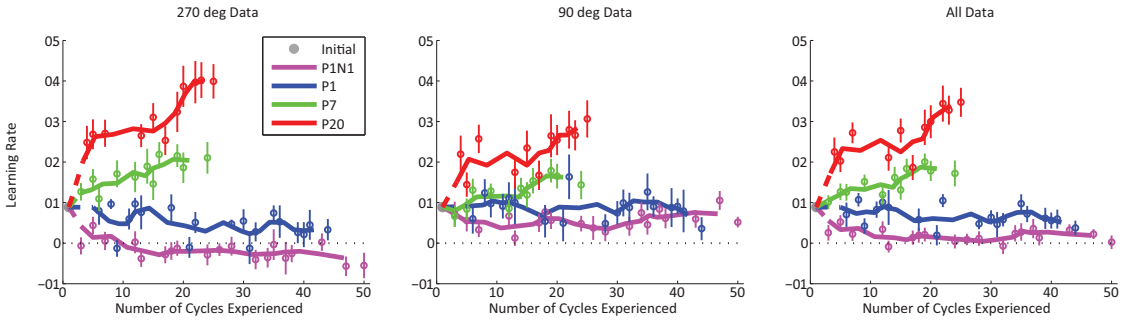

Figure S1. Additional analyses of adaptation rate and washout for the environments presented in Figure 2. Analysis of adaptation data by condition and movement direction. When analyzing the data by condition (P1N1, P1, P7, P20) as well as movement direction with a two-way (condition x movement direction) ANOVA we found a highly significant effect of condition (p = 1.2x10^{-22}, F(3,137) = 52.5) but no overall effect of movement direction (p = 0.57, F(1,137) = 0.33). There was however a moderately significant interaction of condition x movement direction (p = 0.0048, F(3,137) = 4.5). Correspondingly, in this model, the experimental condition effect accounts for 51% of the variance in the data, whereas the interaction effect accounts only for 4%, and the movement direction effect accounts only for 0.1%, indicating that the condition effect dominates. Importantly, both the 270 deg data and the 90 deg data *independently* show a positive relationship between motor adaptation rates and environmental consistency on a one-way ANOVA (p = 1.2x10^{-15}, F(3,69) = 42.4 for the 270 deg data, and p = 4.4x10^{-7}, F(3,68) = 13.7 for the 90 deg data).

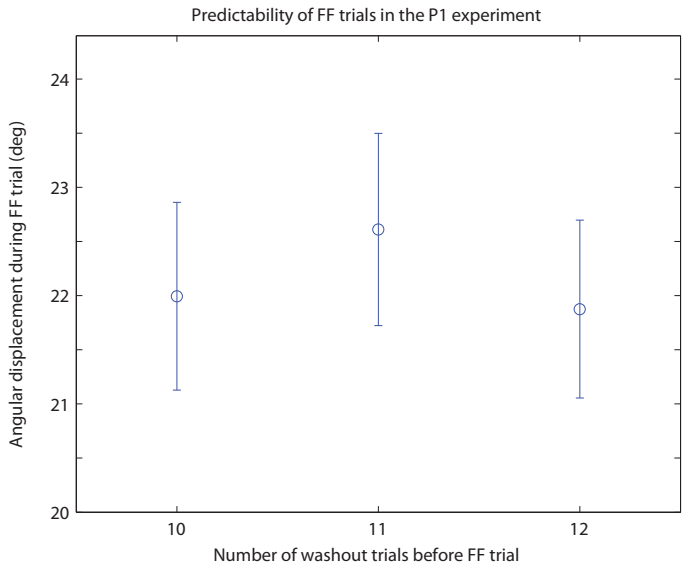

Figure S2. Analysis on the predictability of FF trials in the P1 experiment; related to Figure 2. FF trials following 10, 11, or 12 washout trial display essentially identical displacements (between 21.8 and 22.7 degrees in all cases), and thus there is no significant effect of trial number overall (p = 0.81, F(2,33) = 0.21) and, in particular, the displacements are not significantly different when the FF follows 10 washout trials vs. 12 (p = 0.76), or when the FF follows 10 washout trials vs. 11 (p = 0.23).

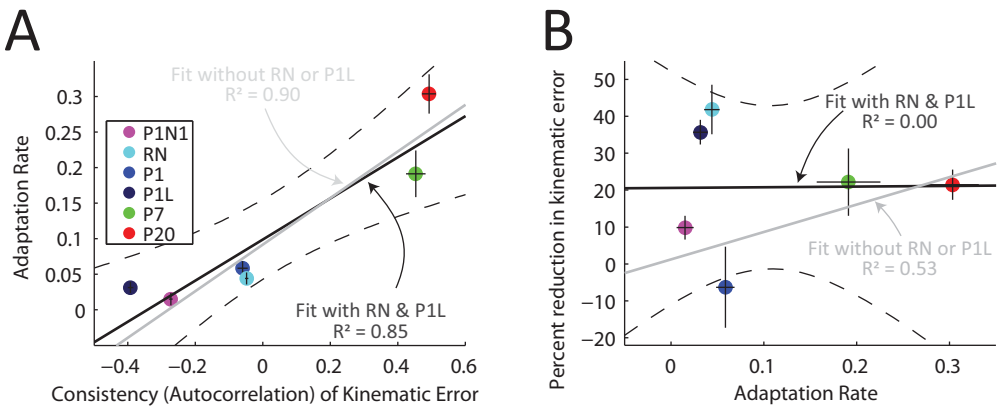

Figure S3. Relationships between adaptation rate, environmental consistency and feedback response strength in our data; related to Figure 3.

(**A**) If instead of analyzing the consistency of the FF in the learning environments as in Figure 3, we look at the consistency of the errors induced by these environments, similar results are obtained. Fit of mean learning rate for all different learning environments as a function of angular error consistency in the environment. Note that both the fits for the P1N1, P1, P7 and P20 data alone (grey solid line) and the fit including the RN and P1L data as well (black solid line) are able to explain a high percentage the variance of the data – 90% ($F(1,2) = 17.49$, $p = 0.053$) and 85% ($F(1,4) = 23.21$, $p = 0.0085$), respectively. The grey dotted line indicates the average initial adaptation rate for all groups and the dashed black curves denote 95% confidence intervals on the overall fit (black solid line). These results suggest that environmental consistency can be estimated by the motor system using either the kinematic errors or forces experienced.

(B) Feedback response strength is plotted as a function of the adaptation rate in each environment, to determine whether these two features of motor control are independent across the experiments in our study. Feedback response strength is measured as the percent reduction in kinematic error for the first FF trial in each block late in learning compared to the initial exposure at the onset of the environment. Note that when fitting for the P1N1, P1, P7 and P20 data alone (grey solid line) a linear fit is able to explain 53% of the variance in the data ($F(1,2) = 2.30$, $p = 0.27$), however, once the RN and P1L results are included and the data are refitted (black solid line) adaptation rate is only able to explain 0% of the variance in the feedback response strength data ($F(1,4) = 0.0006$, $p = 0.98$) indicating that feedback response strength and adaptation rate are independent features in our data set. The black dashed curves denote the 95% confidence intervals on the overall fit (black solid line).

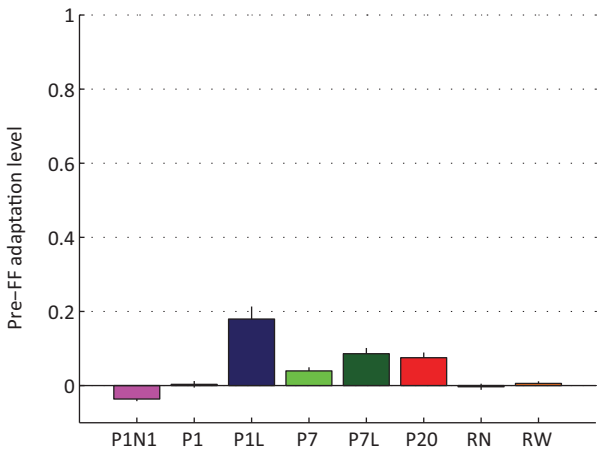

Figure S4. Pre-FF adaptation measurement for each of the eight different environments; related to Figure 3. The plot above shows the adaptation coefficients immediately before the FF trial of each measurement triplet This is the term denoted $x(EC_{pre})$ in Equation 1 in the Experimental Procedures and Equation 2 in the Supplemental Experimental Procedures below. The data shown are from the measurements from the latter half of each environment. Positive adaptation is towards the direction that compensates for the FF which immediately follows these trials. We term this pre-FF adaptation level x_{pre} and note that, if we assume a single-state learning model like the one described in the Introduction (Combined estimation and prediction equation), such a non-zero x_{pre} would bias the corresponding learning rate by an amount equal to $(1-A^2)*x_{pre}$ as suggested by Marko et al. [39] because the adaptation level measured on the post-FF EC trial would be affected by the decay of any pre-FF adaptation as well as the FF-induced learning. However, we chose not to explicitly correct for this effect, because obtaining sufficiently accurate estimates of A would be very difficult and all of our experiments – including RN & RW – were designed in a way that any real bias in our adaptation rate estimates stemming from this effect would be very small.

First, we observe that this value of x_{pre} is negligible for the P1, RN and RW environments. These very small and non-significant values are to be expected, especially for the RN and RW environments: even though the learning measurement triplets in these experiments were not preceded by washout periods, these triplets were: (1) randomly placed in the training period and (2) randomly assigned a sign (positive or negative) for the FF probe trial. This *double randomization* made it highly unlikely for x_{pre} to be consistently biased in the direction of the following FF trial (which would be necessary to a consistent bias).

Second, we observe that, whereas x_{pre} appears statistically significant for the P1N1, P1L, P7, P7L and P20 environments, its corresponding values are rather small. The small values for x_{pre} in these blocked paradigms mean even smaller values for $(1-A^2)*x_{pre}$. It is interesting to note that $(1-A^2)*x_{pre}$ would almost always be small for blocked paradigms with washout periods before each measurement triplet, because a value of A substantially lower than 1 would insure a fairly rapid decay of adaptation prior to x_{pre}, leading to a very small value for x_{pre} itself. However, values of A close to 1, which may allow x_{pre} to be of reasonable amplitude would insure that the term $(1-A^2)$ is small, which would in turn result in a small value for the $(1-A^2)*x_{pre}$ bias even if x_{pre} were not very small. It is worth mentioning that the P1L group shows an x_{pre} bias that is more than twice as high as any of the other groups, but still only 0.18 in size. This makes sense because we were forced to substantially abbreviate the washout period for this group in order to fit the 540 cycles that this experiment required into a single (3.5 hour) session (and neither of the randomizations we used in the RN & RW experiments could be employed). We estimated the bias that would be associated with the P1L experiment, which has the largest x_{pre} value. To do so, we coupled the "forward" bias equation $(1-A^2)*x_{pre}$ with the corresponding "reverse" equation in order to obtain a system of two equations and two unknowns that allows for A to be estimated and thus the bias $(1-A^2)*x_{pre}$ to be approximated. By the "reverse" equation, we mean the state-space equation analogous to the forward one given above that instead describes the propagation of learning from the last trial of a triplet (the post-FF EC trial) to the first trial of the following triplet (the pre-FF EC trial). In so doing, we estimated the bias $(1-A^2)*x_{pre}$ to be about 0.01 which is indeed rather small.

A critical technical issue with the specific $(1-A^2)*x_{pre}$ bias correction is that it assumes 1-rate learning which is unlikely. *The practical issue here is that, especially for the one-sided blocked paradigms with washout periods used in many of our experiments, $x_{pre}=x_{pre,SLOW}+x_{pre,FAST}$ is likely to be dominated by slow learning, i.e. $x_{pre,SLOW} >> x_{pre,FAST}$ (because fast learning would decay and be washed out much more quickly during the washout period, allowing only slow learning to possibly accumulate from one one-sided block to the next).* Thus the overall decay bias would in fact have two components: $(1-A_{FAST}^2)*x_{pre,FAST} + (1-A_{SLOW}^2)*x_{pre,SLOW}$. However, if decay is measured directly in a single trial

following adaptation, as in [39], where the $(1-A^2)*x_{pre}$ bias correction is used, the estimated value for A would be approximately A_{FAST} (as also admitted in [39]), because in contrast to x_{pre} most of the learning following single-trial adaptation would be fast. Correspondingly, the $(1-A^2)*x_{pre}$ bias correction would do more harm than good if most of x_{pre} was from $x_{pre,SLOW}$ (i.e., if $x_{pre,SLOW} > x_{pre,FAST}$ as it almost certainly will be), because the $(1-A^2)*x_{pre}$ bias correction would effectively apply A_{FAST} to the decay of both $x_{pre,FAST}$ and $x_{pre,SLOW}$ (the latter of which would dominate and would be expected to, practically speaking, not decay at all since $A_{SLOW} > 0.99$ → less than 1% decay per trial). By "more harm than good" we mean that the "corrected" estimate of learning would be farther away from the true learning than the "uncorrected" estimate was. Thus we would maintain that the $(1-A^2)*x_{pre}$ bias correction should only be considered if there is a reasonable expectation that $x_{pre,FAST} >> x_{pre,SLOW}$, which is not likely to be the case for our blocked experiments. Moreover, we would suggest that it is unclear whether this condition is likely to be met for the data in the Marko et al. [39] study where this correction was implemented, raising the issue of whether the $(1-A^2)*x_{pre}$ correction did more harm than good in that study.

We did however, make use of the pre-FF adaptation level measurements above to refine our measurements of feedback response strength. The idea here is that $F_{perturb}-x_{pre,raw}$ would be a better estimate of the environmental perturbation on a given trial than $F_{perturb}$ alone. Thus, we normalized the kinematic errors used to compute feedback response strength by $F_{perturb}-x_{pre}$ rather than $F_{perturb}$ alone (note that, practically speaking this entailed normalization of the current kinematic error estimates by $1-x_{pre}$, as learning coefficients like x_{pre} in the paper are normalized by $F_{perturb}$ and $F_{perturb}/(F_{perturb}-x_{pre,raw}) = 1/(1-x_{pre,raw}/F_{perturb}) = 1/(1-x_{pre})$) – also see Supplemental Experimental Procedures below. The small values of x_{pre} we observe predict that the effect is small, but we felt that accounting for it might further improve the accuracy of our feedback response rate estimates.

Supplemental Tables

Table S1. Group Mean and Individual Subject Data Analyses, related to Figure 3.
Note that NS indicates not significant at $\alpha = 0.05$.

Fit For		Group Mean Data		Individual Subject Data	
		R^2	*p*-value	R^2	*p*-value
Adaptation Rate vs. Consistency of FF	W/O RN/P1L Data	0.94	0.030	0.60	3.3×10^{-15}
	With RN/P1L Data	0.90	0.004	0.62	4.3×10^{-21}
Adaptation Rate vs. Variance of FF	W/O RN/P1L Data	0.69	0.17 (NS)	0.45	1.3×10^{-10}
	With RN/P1L Data	0.16	0.43 (NS)	0.19	9.9×10^{-6}
% Reduction in KE vs. Consistency of FF	W/O RN/P1L Data	0.58	0.24 (NS)	0.09	0.012
	With RN/P1L Data	0.00	0.99 (NS)	0.00	0.78
% Reduction in KE vs. Variance of FF	W/O RN/P1L Data	0.95	0.024	0.17	0.00059
	With RN/P1L Data	0.82	0.013	0.24	1.0×10^{-6}

Table S2A. Bi-variate regression of **adaptation rate** onto both consistency and variance using **group mean data** (all groups) compared to univariate regressions. Related to Figure 3.

	Regression onto Consistency of FF	Regression onto Variance of FF	Regression onto both Consistency and Variance of FF	
			Consistency of FF	Variance of FF
Coefficients ($\beta \pm$ 95% C.I.)	0.20 ± 0.09	0.0032 ± 0.010	0.19 ± 0.13	0.0004 ± 0.0050
R^2 or partial R^2	$R^2 = 0.90$	$R^2 = 0.16$	$R_c^2 = 0.88$	$R_v^2 = 0.022$
F-statistic	F(1,4) = 35.32	F(1,4) = 0.76	F(1,3) = 22.3	F(1,3) = 0.068
p-value	0.004	0.43	0.018	0.81

Table S2B. Bi-variate regression of **adaptation rate** onto both consistency and variance using **individual subject data** (all groups) compared to univariate regressions. Related to Figure 3.

	Regression onto Consistency of FF	Regression onto Variance of FF	Regression onto both Consistency and Variance of FF	
			Consistency of FF	Variance of FF
Coefficients ($\beta \pm$ 95% C.I.)	0.22 ± 0.035	0.0051 ± 0.0022	0.21 ± 0.041	-0.0006 ± 0.0017
R^2 or partial R^2	$R^2 = 0.62$	$R^2 = 0.19$	$R_c^2 = 0.51$	$R_v^2 = 0.0048$
F-statistic	F(1,93) = 149.9	F(1,93) = 21.86	F(1,92) = 95.82	F(1,92) = 0.44
p-value	4.3×10^{-21}	9.9×10^{-6}	$< 10^{-15}$	0.51

Table S3A. Bi-variate regression of **feedback response strength** (% reduction in kinematic error) onto both consistency and variance using **group mean data** (all groups) compared to univariate regressions. Related to Figure 3.

	Regression onto Consistency of FF	Regression onto Variance of FF	Regression onto both Consistency and Variance of FF	
			Consistency of FF	Variance of FF
Coefficients ($\beta \pm$ 95% C.I.)	-0.01 ± 43.64	1.09 ± 0.71	-12.44 ± 13.70	1.26 ± 0.52
R^2 or partial R^2	$R^2 = 0.00$	$R^2 = 0.82$	$R_c^2 = 0.74$	$R_v^2 = 0.95$
F-statistic	F(1,4) = 0.00	F(1,4) = 17.88	F(1,3) = 8.34	F(1,3) = 59.03
p-value	0.99	0.013	0.063	0.0046

Table S3B. Bi-variate regression of **feedback response strength** (% reduction in kinematic error) onto both consistency and variance using **individual subject data** (all groups) compared to univariate regressions. Related to Figure 3.

	Regression onto Consistency of FF	Regression onto Variance of FF	Regression onto both Consistency and Variance of FF	
			Consistency of FF	Variance of FF
Coefficients ($\beta \pm$ 95% C.I.)	1.48 ± 10.32	1.01 ± 0.38	-13.81 ± 10.04	1.29 ± 0.42
R^2 or partial R^2	$R^2 = 0.00$	$R^2 = 0.24$	$R_c^2 = 0.078$	$R_v^2 = 0.30$
F-statistic	F(1,89) = 0.08	F(1,89) = 27.62	F(1,88) = 7.47	F(1,88) = 36.9
p-value	0.78	1.0×10^{-6}	0.0076	3.00×10^{-8}

Supplemental Experimental Procedures:

Ethics statement

All experimental participants were naïve to the experimental purpose, provided informed consent and were compensated for their participation. All the experimental protocols were reviewed and approved by the Harvard University Committee on the Use of Human Subjects (CUHS) in research.

General task description

Subjects performed 10cm reaching movements in the horizontal plane with their dominant hands while grasping the handle of a 2-link robotic manipulandum, Figure 1A. They were presented with 1cm-diameter circular targets displayed on a vertically oriented LCD monitor. The position of the subject's hand was represented on the LCD monitor by a 3mm cursor. Position, velocity and force at the handle were measured with sensors installed in the manipulandum at a sampling rate of 200Hz. The subjects were instructed to produce fast, continuous movements, and were provided visual feedback throughout the movement. Feedback about the movement time achieved was presented at the end of each movement. Ideal movement times (500±50ms) were signaled by an animation of the target while a chirp sound was played. Here movement time on each trial was defined that the time between when the movement speed first exceeded 0.05m/s and the final time it went below 0.05m/s. For movement completion times that were below or above the ideal range the targets were colored blue and red, respectively and the chirp sound was withheld. The mean peak speed for the movements in all experiments was 0.33±0.04m/s. All movements in the present study occurred in the 90º and 270º directions (Figure 1A). In certain movements, the subjects' trajectories were disrupted by velocity-dependent dynamics. This was implemented by a viscous curl force-field (FF) at the handle produced by the motors of the manipulandum, Equation 1 and Figure 1B.

(1) $$\vec{F}(\vec{v}) = B\vec{v} = \begin{bmatrix} 0 & b \\ -b & 0 \end{bmatrix} \begin{bmatrix} v_x \\ v_y \end{bmatrix}$$

In this equation the constant 2 x 2 matrix B represents the viscosity associated with this FF. In particular, we constrained B so that it had a curl matrix form with amplitude b as shown above. This curl form resulted in the direction of the force always orthogonal to the direction of the velocity vector. In most of the experiments (P1N1, P1, P1L, P7, P7L and P20) the magnitude of the

scalar b was set to 15 N/(m/s) and its sign was set so that half of the subjects experienced a clockwise FF (b=+15 N/(m/s)) while the other half experienced a counterclockwise FF (b =-15 N/(m/s)) during training. In these experiments, the FF blocks or single trials began with movements in the 270º direction. In the RN and RW environments the mean value of b was approximately zero but its specific value was changed from one trial to the next as described below.

We assessed the level of adaptation using error-clamp trials, i.e., we measured the force pattern that subjects produced when their lateral errors were held to near zero values in an error-clamp [14, 36-37], Figure 1B. We then regressed the ideal force required to fully compensate the force-field onto these measured force patterns. The slope of this regression was used as the adaptation coefficient (x) that characterized adaptation in that trial. Note that the mean force patterns as well as the corresponding adaptation coefficients are shown in Figures 2-5.

Measures of feedforward learning and feedback control

In all experiments, we measured feedforward adaptation based on the lateral force output observed during error clamp trials. Compared to kinematic measures of learning, this force-based measure can be more directly compared to the force-based nature of the environments we employed, and it is unaffected by limb stiffness. In particular, the adaptation rates reported in this study were calculated by obtaining the difference between the adaptation coefficient for the error-clamp trial following the first FF trial in a measurement cycle (EC_{Post}) and the adaptation coefficient for the error-clamp trial preceding this force-field trial (EC_{Pre}), Equation 2 and Figure 1B.

(2) $$Adaptation\ Rate = x(EC_{Post}) - x(EC_{Pre})$$

The percent reduction in kinematic error in a given FF trial (e_{FF}) compared to the kinematic error in the first presentation of the FF (e_{Init}) was calculated by subtracting e_{FF}, corrected to account for the amount of adaptation in the preceding trial, from e_{Init}, and normalizing by (e_{Init}), as shown in Equation 3 for all experiments. As adaptation directly leads to corrections in error that are independent of stiffness, we corrected the kinematic error in a given FF trial (e_{FF}) for the amount of adaptation in the preceding trial by normalizing e_{FF} by the corresponding gap in adaptation (i.e. the adaption shortfall), $1 - x(EC_{Pre})$.

(3) $$\%\ Reduction\ in\ kinematic\ error = \frac{e_{Init} - \frac{e_{FF}}{1 - x(EC_{Pre})}}{e_{Init}}$$

Learning environment experiments: definitions of consistency and variability

Different learning environments were created to study the environmental modulation of adaptation rate in different experiments, Figure 1B. We operationally defined environmental consistency is defined as the lag-1 autocorrelation (R(1)) of the FF sequence, i.e., the expected value of the covariance of the magnitude of the force between the current trial and the subsequent trial in the same movement direction, normalized by the overall variance of the force-field environment, Equation 4.

(4) $$Consistency: R(1) = \frac{E[(FF_n - \mu_{FF})(FF_{n+1} - \mu_{FF})]}{\sigma_{FF}^2}$$

We note that for all environmental consistency and variability calculations, we used the adaptation coefficient *x* as a measure of the effective FF strength for error clamp trials, because in the robotic manipulandum produced a force that matched the adapted motor output in each error clamp trial.

Learning environment experiments: paradigm details

Note that all experiments began with a 200-trial baseline/familiarization period before the environment being studied was applied. Note also that all blocked experiments were balanced in terms of FF direction with half of the subjects experiencing clockwise curl FFs and the other half experiencing counterclockwise curl FFs.

In the anti-consistent learning environment (P1N1; $R(1)$=-0.3) experiment, 21 subjects (mean age=20.7 ± 2.5 years; 7 male) completed two baseline blocks of null movements (100 movements/block) in the 90º/270º directions to obtain familiarity with the task. The subjects were then exposed to 50 environment cycles where they experienced the following sequence of trials in each movement direction: a single positive FF trial (b=15 N/(m/s)), followed by a single negative FF trial (B=-15 N/(m/s)), followed by 11-13 washout (null) trials. To assess the adaptation rate of the subjects we randomly interspersed error-clamp trials before and after the positive FF trial in a subset of the FF cycles (40%) with the aforementioned sequence. The adaptation rate was calculated as described above for both the 90º and 270º directions.

In the inconsistent learning environment (P1; $R(1)$=-0.05) experiment, 12 subjects (mean age=23.8 ± 6.6 years; 1 male) were exposed to two baseline blocks of null movements (100

movements/block) in the 90º/270º directions to obtain familiarity with the task. The subjects were then exposed to 45 environment cycles where they experienced the following sequence of trials in each movement direction: a single positive FF trial (b=15 N/(m/s)), followed by 10-12 washout (null) trials. Randomly interspersed in a subset of the environment FF cycles (44%) we introduced error-clamp trials before and after the positive FF trial of the aforementioned sequence to assess the subjects' adaptation rate. This process was applied to both the 90º and 270º directions.

In the medium consistency learning environment (P7; $R(1)$=0.74) experiment, 12 subjects (mean age=23.8 ± 6.6 years; 1 male) completed two baseline blocks of null movements (100 movements/block) in the 90º/270º directions to obtain familiarity with the task. The subjects were then exposed to 27 environment cycles where they experienced the following sequence of trials in each movement direction: seven positive FF trials (b=15 N/(m/s)), followed by 15-18 washout (null) trials. Randomly interspersed in a subset of the environment cycles (44%) we introduced error-clamp trials before and after the first FF trial of the aforementioned sequence to assess the subjects' adaptation rate. This process was applied to both the 90º and 270º directions.

In the high consistency learning environment (P20; $R(1)$=0.90) experiment, 28 subjects (mean age=22.8 ± 3.9 years; 15 male) completed two baseline blocks of null movements (100 movements/block) in the 90º/270º directions to obtain familiarity with the task. The subjects were then exposed to 27 environment cycles where they experienced the following sequence of trials in each movement direction: twenty positive FF trials (b=15 N/(m/s)), followed by 28-32 washout (null) trials. Randomly interspersed in a subset of the environment cycles (44%) we introduced error-clamp trials before and after the first FF trial of the aforementioned sequence to assess the subjects' adaptation rate. In addition, for 16 out of these 28 subjects, at the end of the last FF environment cycle we added a single negative FF trial, surrounded by EC trials, to assess the adaptation rate associated with this novel perturbation. This was done for both the 90º and 270º movement directions.

A group of 18 subjects (mean age=20.3 ± 2.7 years; 6 male) completed an extended version of the medium consistency learning environment experiment (P7L; $R(1)$=0.73), modified to include the approximately the same number of FF trials used in the high consistency learning environment experiment (P20) – 539 FF trials in P7L vs 540 FF trials in P20. These subjects completed 2 blocks of 100 null familiarization trials in the 90º/270º directions, and then 77 environment cycles where they experienced the following sequence of trials in each movement direction: seven positive FF

trials (B=15 N/(m/s)), followed by 10-14 washout (null) trials. Randomly interspersed in a subset of the environment cycles (45%) we introduced error-clamp trials before and after the first positive FF trial of the aforementioned sequence to assess the subjects' adaptation rate. In addition, at the end of the last FF environment cycle we added a single negative FF trial, surrounded by EC trials, to assess the adaptation rate associated with this novel perturbation. This process was applied to both the 90º and 270º directions.

A group of 12 subjects (mean age=21.8 ± 2.9 years; 4 male) completed an extended version of the inconsistent learning environment experiment (P1L; R(1)=-0.45), modified to include the same number of FF trials (540) used in the high consistency learning environment experiment (P20). These subjects completed 2 blocks of 100 null familiarization trials in the 90º/270º directions, and then 540 environment cycles where they experienced the following sequence of trials in each movement direction: one positive FF trials (b=15 N/(m/s)), followed by 1-3 washout (null) trials. Randomly interspersed in a subset of the environment cycles (22%) we introduced error-clamp trials before and after the first positive FF trial of the aforementioned sequence to assess the subjects' adaptation rate. The adaptation rate was calculated by subtracting the adaptation coefficient in the first EC trial from the adaptation coefficient in the second EC trial. This process was applied to both the 90º and 270º directions.

In the random noise learning environment (RN; R(1)=0.02) experiment, 13 subjects (mean age=22.4 ± 3.5 years; 8 male) were exposed to two baseline blocks of null movements (100 movements/block) in the 90º/270º directions to obtain familiarity with the task. The subjects were then exposed to an environment where the FF trials varied randomly, with magnitudes determined according to a normal distribution with standard deviation of 7.5 N/(m/s). Randomly interspersed in this environment we introduced error-clamp trials (1% of trials) to assess the adaptation rate of the subjects according to the following sequence of trials, (1) EC trial, (2) FF trial of magnitude ± 15 N/(m/s), (3) EC trial, Figure 1B. The adaptation rate was calculated by subtracting the adaptation coefficient in the first EC trial from the adaptation coefficient in the second EC trial. This process was applied to both the 90º and 270º directions.

Finally, in the random walk learning environment (RW; R(1)=0.76) experiment, 23 subjects (mean age=22.4 ± 3.5 years; 10 male) were exposed to two baseline blocks of null movements (100 movements/block) in the 90º/270º directions to obtain familiarity with the task. The subjects were

then exposed to an environment where the strength of the viscous FF followed a damped random walk:

$$b(k) = Ab(k-1) + w(k)$$

Where $b(k)$ is the strength of the force-field at trial k, $A = 0.88$ was the carryover (retention) coefficient and $w(k)$ was zero-mean random noise with a standard deviation of 2.7 N/(m/s), chosen so that the variance of the overall environment roughly matched the variance of the random noise environment. Note that this is similar to a regular (undamped) random walk for which A would be 1. We used a value for the carryover coefficient (A) smaller than 1 to ensure that the amplitude of b does not grow unbounded. Note that this value is numerically equal to the expected value of the lag-1 autocorrelation ($R(1)$) for an infinitely long sequence $b(k)$. EC-FF-EC measurement triplets, like those described above, were randomly interspersed in this environment with a mean interval of 30 trials to measure the adaptation rate in both the 90º and 270º directions. The perturbation trial in the triplet had a b of +15Ns/m in half the triplets and -15Ns/m for the other half. Note that without interspersing these triplets the $R(1)$ for the RW environment would be close to $A = 0.88$; however, the fact that the FF perturbations contained within these triplets are uncorrelated to the FF trials that precede or follow them reduces the lag-1autocorrelation from 0.88 to $R(1) = 0.76$. The amplitude of the FF coefficient b was capped at 24Ns/m.

Data inclusion criteria

In our data analysis grossly irregular trials were excluded. This included movements that were extremely fast (peak velocity > 0.5 m/s) or extremely slow (peak velocity < 0.22 m/s), as well as trials with extremely fast (< 75 ms) or extremely slow (> 2.5 sec) reaction times. This insured that subjects did not initiate movements too quickly, without correctly identifying the location of the target, or too late, indicating that they might have not been attending to the task. Applying these criteria resulted in the inclusion of at least 90% of the trials in each group: 94% in the P1N1 group, 90% in the RN group, 97% in the P1 group, 94% in the P7 group, 93% in the P7L group, and 91% in the P20 group. Furthermore, we excluded from our analyses subjects for which less than one third of their EC triplet data fit the inclusion criteria within the number of trials analyzed. Specifically, from the analyses of the latter half of the data (Figures 2BC, 3 and 5 and Figure 6), 7 subjects were excluded: one from the P7 environment, one from the P20 environment, one from the RN environment and four from the RW environment. From our analysis of the last third of the data (Figure 4B) the same two subjects from the P7 and P20 environments were excluded.

Statistical analyses

Differences in kinematic error during training between the learning environments were assessed with a one-way analysis of variance (ANOVA). We also used ANOVAs to assess differences in initial (first measurement sequence) and late (last half of measurement sequences) adaptation rate and percent reduction in kinematic error between the learning environments. Notice that the number of degrees of freedom (DOF) of the error in the comparison of initial adaptation rate is 66 and not 69 because trials from 3 subjects – one in the P1, one in the P7 and one in the P20 groups – failed at least one of the data inclusion criteria noted above. When significant differences arose in the ANOVAs, hypothesis-based post-hoc comparisons were performed using one-tailed *t*-tests. Comparisons between pairs of groups were performed using unpaired *t*-tests without the assumption of equal variances between groups, whereas within group comparisons were performed using paired *t*-tests.

Calculation of confidence intervals for the responses predicted by the combined-CR model

As the combined-CR prediction for the P7L-Opposite response was based on data from different subject populations (RW and P7L, since the prediction was equal to -RW+(P7L-RW)) we could not directly measure variability across subjects to determine SEM as is the other analyses presented in the paper. Thus we utilized a bootstrapping procedure in order to estimate the SEMs associated with this combined-CR prediction (displayed in Figure 6C). Specifically, we repeatedly randomly sampled with replacement from the RW and P7L subject populations for a total of 10,000 iterations, and used the standard deviation of the corresponding sample averages as a measure of SEM. The same process was used for the combined-CR prediction for the P20-Opposite response (Figure 6D).

Supplemental References:

39. Marko, M.K., Haith, A.M., Harran, M.D., and Shadmehr, R. (2012). Sensitivity to prediction error in reach adaptation. J. Neurophysiol. *108*, 1752-1763.